OBSERVATION OF LAMINAR MIXING STRUCTURES IN A PERTURBED TAYLOR VORTEX FLOW

Tsukasa Makino, Takuya Kaise, Kenji Sasaki, Naoto Ohmura*, and Kunio Kataoka

[1]Department of Chemical Science and Engineering, Kobe University,
Rokkodai, Nada, Kobe 657-8501, Japan
*Corresponding author: Naoto Ohmura, ohmura@cx.kobe-u.ac.jp

Abstract

The purpose of the present work is to observe laminar mixing structures in a periodically perturbed Taylor vortex flow system with the aspect ratio Γ = 2. In the range less than *Re* = 200, isolated mixing regions (IMRs) took clearly the form of two toroidal vortices in the upper and lower circulating flows, respectively. A couple of simple core tori were observed in the case when using the rotating inner cylinder with smooth surface, while a set of some thin tori spirally wrapping around the core of each IMR were observed in the case when using the cylinder having protrusions on the surface. It was found that different numbers of tori were obtained for different numbers of protrusions, even at nearly the same Reynolds numbers. Hence it can be considered that the structure of the IMRs depends on periodical perturbations generated by the passing protrusions of the rotating inner cylinder.

Introduction

Mixing is one of the most important operations in industrial chemical processes. A wide variety of mixing equipment is commercially available in a wide variety of impeller configurations, size and operation. Especially, a stirred vessel is one of the most frequently used mixing apparatuses. Owing to its versatility, it can be operated under a wide range of condition for a wide variety of fluids. Consequently, mixing in a stirred vessel is often conducted under low Reynolds number conditions. The low Reynolds number flow conditions often bring inefficient global mixing owing to the organized core structures, called isolated mixing region (IMR) [1]. A couple of IMRs comprise two toroidal vortex cores formed respectively above and below an impeller. They do not exchange much fluid material with the outside active mixing region (AMR). They can often serve as a substantial obstacle to global mixing. It is important to elucidate the structure of the IMRs in order to precisely control them. However, it is rather complicated to analyze their flow structure owing to non-uniformity of centrifugal force and of perturbation effect by an impeller in the axial direction.

In a Taylor vortex flow system, there appear pairs of counter-rotating toroidal vortices spaced regularly along the cylinder axis. This circulatory flow pattern is quite similar to that in a stirred vessel. This flow system also has isolated mixing regions within toroidal vortices in the laminar Taylor vortex flow regime [2]. The Taylor vortex flow can be regarded as simplification of a flow model in a stirred vessel. The purpose of the present work is to observe laminar mixing structures in a Taylor vortex flow system periodically perturbed by protrusions on the surface of the rotating inner cylinder with the aspect ratio Γ = 2.

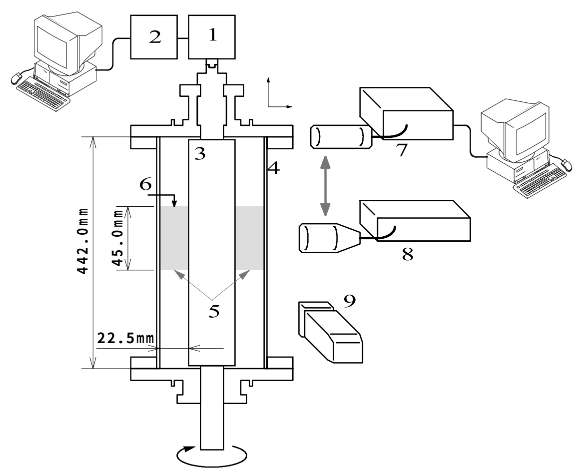

Fig. 1 Experimental apparatus with measuring system: 1 motor, 2 controller, 3 inner cylinder, 4 outer cylinder, 5 test section, 6 tracer injector, 7 LDV system, 8 Ar laser system, and 9 digital video camera

Experiment

The experimental apparatus with measuring system is shown in Fig. 1. The experimental apparatus consisted of a transparent outer cylinder of acrylic resin (120 mm ID) and an inner cylinder of

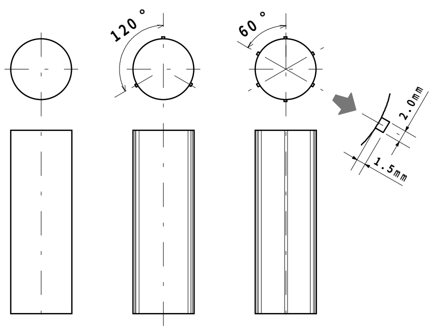

Fig. 2 Protrusions fixed on the outer surface of the inner cylinder

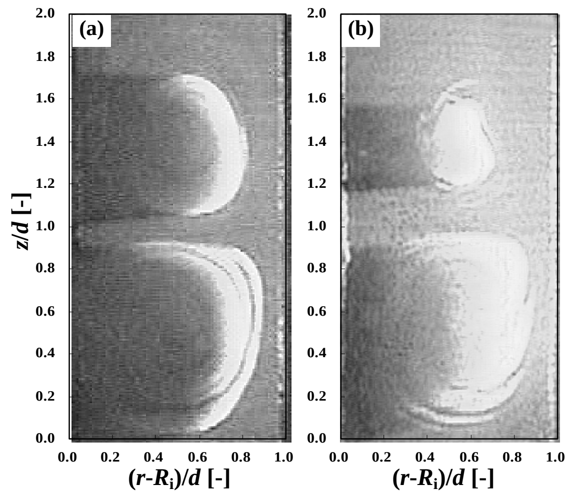

Fig. 3 Cross sectional views of the IMRs: (a) inner cylinder A (*Re*=51.9) and (b) inner cylinder B (*Re*=167.3).

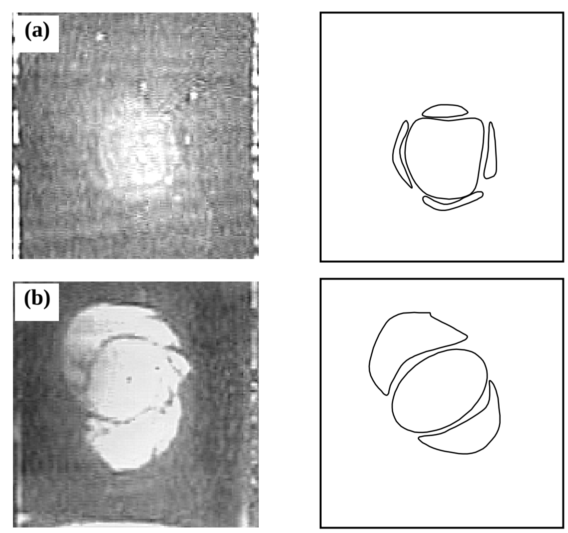

Fig. 4 Photographs and schematic diagrams of the upper IMRs formed using inner cylinder B: (a) *Re*=125.7 and (b) *Re*=79.4.

stainless steel (75 mm OD), giving an annular gap width *d* of 22.5 mm. The annular space was divided into three potions with two partition discs (2 mm thick). The test section was the central portion having an aspect ratio Γ (= H/d) = 2.0 so as to confine two vortex cells in normal flow conditions. As shown in Fig. 2, three kinds of inner cylinders were used: A = smooth surface with no protrusion, B = three protrusions arrayed at every 120 ° and C = six protrusions arrayed at every 60 ° . Aqueous solution of glycerin was used as the working fluid. In order to eliminate photographic distortion, the test section was surrounded with a square-shaped vessel filled in the same fluid as the working fluid. Fluorescent pH-sensitive neutrally-buoyant green dye was used as a passive tracer. The working fluid was initially made basic by adding a small amount of basic solution consisting of 0.5 N NaOH and aqueous solution of glycerin. After the inner cylinder reached a certain rotational speed with the acceleration rate of 0.05 1/s, a small amount of acidic solution (0.5 N HCl and glycerin) was carefully added from the top of the test section so as to decolorize the green dye due to the neutralization reaction. A couple of IMRs could be discerned as the colored regions remaining unchanged in the vessel. The IMRs were induced to fluoresce using a plane sheet of Ar-laser light. The sequential digital images of the decolorization process were taken using a digital video camera. Three components of local velocities were measured by a laser-Doppler velocimeter (LDV).

Results and discussion

Fig. 3 (a) and (b) show typical cross-sectional views of the upper and lower IMRs observed using the inner cylinders with and without 3 protrusions, respectively. The IMRs took clearly the form of two toroidal vortices in the upper and lower circulating flows in the both cases. These regions could be seen when Re (= $R_i \omega d/\nu$) ≤ 200, and they remained visible 20 – 60 min, where R_i is radius of the inner cylinder, ω is angular velocity of the inner cylinder and ν is kinematic viscosity. Owing to the location of tracer injector, decolorization firstly occurred in the upper vortex. In Fig. 3, therefore, the upper IMR takes a final steady structure, while the lower one is still in a transient state. As can be seen from Fig. 3 a), the surfaces of IMRs are smooth. This indicates that each IMR consists of a simple core torus. Only this simple

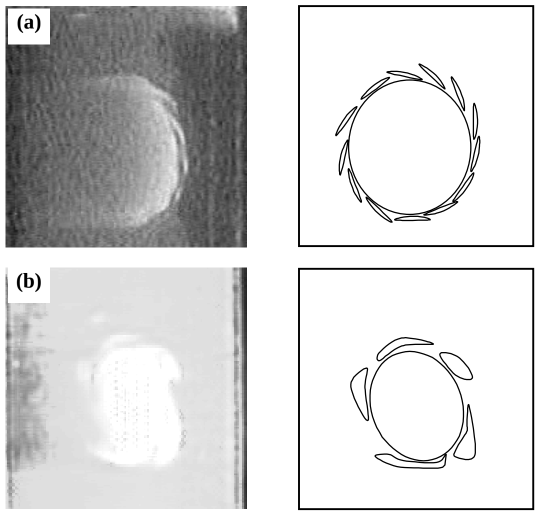

Fig. 5 Photographs and Schematic diagrams of the upper IMRs formed using inner cylinder C: (a) *Re*=123.5 and (b) *Re*=190.6.

core torus could be seen in a range of *Re* = 50 – 150 in the case when using cylinder A (no protrusion). On the other hand, three stable islands rounding around the core torus could be seen in the cross-sectional view. These results suggest that periodical perturbations imposed due to protrusions on the circulatory streamlines generate the island structure.

Fig. 4 shows photographs and schematic diagrams of cross-sectional views of the upper IMR for two different Reynolds numbers in the case when using the inner cylinder B (3 protrusions). As can be seen from Fig. 4 (a), the core torus is surrounded with four islands. These islands moved around the core torus with a certain period. This means that the IMRs have multi structures consisting of various Kolmogorov-Arnold-Moser (KAM) tori. The experiment revealed that normally the number of islands decreased with increasing the Reynolds number. This result was confirmed by our previous work [3] using a stirred vessel. However, an exceptional structure was observed in the present work. At *Re* = 79.4 (Fig. 4 (b)), two islands were observed. These islands were crescent-shaped and larger than the core torus. Furthermore, they did not move around the core torus. This structure of the islands is quite similar to the numerical result by Broomhead and Ryrie [4]. Fig. 5 also shows photographs and schematic diagrams of cross-sectional views of the upper IMR for two different Reynolds numbers in the case when using the inner cylinder C (6 protrusions). In the 6-protrusion case, only the moving island structure could be seen. At *Re* = 123.5, more than ten islands could be observed.

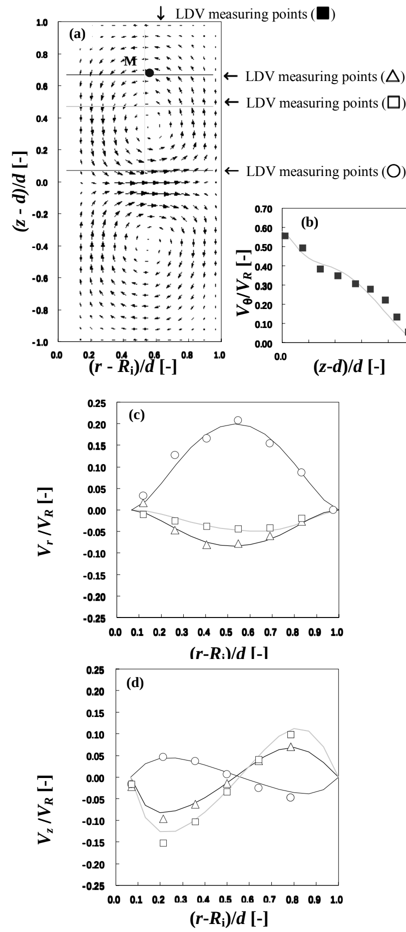

Fig. 6 Relationship between numerical and experimental velocity field (*Re*=190.9): (a) velocity vector distribution, (b) tangential velocity, (c) radial velocity and (d) vertical velocity.

In comparison with Fig. 4 (a), the number of islands was larger than that in the case of 3-protrusion, even at nearly the same Reynolds numbers, i.e. nearly the same rotational speeds of inner cylinder. Fig. 6 shows velocity distributions at *Re* = 190.9 in the 6-protrusion case in comparison with those without protrusion obtained by three-dimensional numerical simulations based on the method of the forward time integration scheme combined with the central finite difference method for spatial discretization [5]. A good agreement between experimental and numerical results can be seen. This indicates that the protrusion did not affect on the mean velocity field. It can be, therefore, considered that different number of islands for different number of protrusions even at nearly the same Reynolds numbers is mainly due to the perturbation frequency given by the passing protrusions.

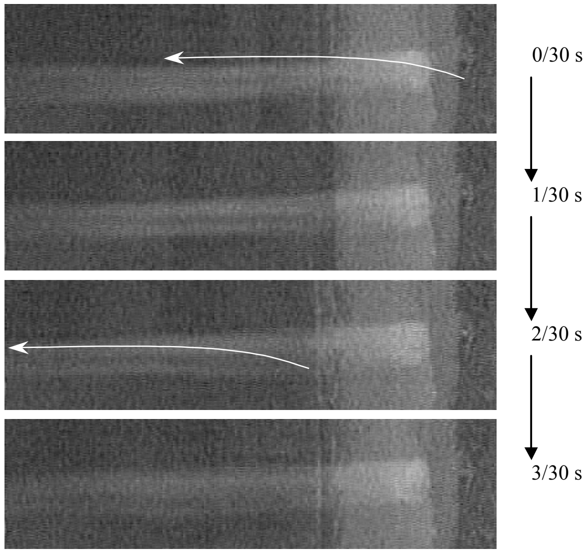

Fig. 7 Geometrical structure and motion of thin torus (inner cylinder C: *Re* = 190.6)

Fig. 7 shows a global structure of the IMR. This figure indicates in the three-dimensional view that normal islands appear in the form of thin tori spirally wrapping around the core of the IMR. Lamberto et al. [1] called this thin torus as "filament". They also predicted similar structures in a stirred vessel and they called this structure as "clay model". In our previous work [3] using a stirred vessel, however, no spirally wrapping structure appeared and the small tori simply moved around the core torus repeatedly stretching and contracting. These results suggest that the geometrical structure of the IMRs largely depends on the type of perturbation.

The above results might be better understood by applying the Poincaré-Birkhoff theorem in the nonlinear dynamic theory [6]. This theorem states: 1) If the circulation time period on a periodic orbit is n times as long as the perturbation period, $2n$ fixed points are generated, where n is an integer. 2) Among these $2n$ fixed points, n points are unstable hyperbolic points while the other n points are stable elliptic points. 3) These hyperbolic and elliptic points circularly get lined up in turns. In practice, the unstable hyperbolic fixed points are invisible and only the stable elliptic points can be seen. This theorem cannot directly be applied to this flow system because it is applicable for a time-dependent two-dimensional flow system. It can be conjectured that the island structures are formed around these stable elliptic fixed points on a rational orbit. With the aid of nonlinear dynamic theory, it might be possible to precisely control the structure of the IMRs by varying the shape of impellers in an industrial stirred vessel.

Conclusions

The following conclusion has been made:

1) Isolated mixing regions have complex multi-structures consisting of various KAM tori in the case when using the inner cylinder with protrusions.
2) Normally, a set of some thin tori appear spirally wrapping around the core of each IMR and they move around with a certain period.
3) The structure of the IMRs depends on periodical perturbations generated by the protrusions fixed on the rotating inner cylinder.
4) With the aid of nonlinear dynamic theory, it might be possible to precisely control the structure of the IMRs by varying the shape of impellers in an industrial stirred vessel.

Acknowledgements

The authors wish to thank Dr. T. Takigawa and Mr. T. Yoshimura for their experimental support. This research was financially supported by a Grant-in-Aid for Encouragement of Young Scientists (No. 12750663) from the Ministry of Education, Science, Sports and Culture of Japan.

References

[1] Lamberto, D. J., Muzzio, F. J., Swanson, P. D. and Tonkovich, A. L., 1996, "Using time-dependent RPM to enhance mixing in stirred vessel," Chem. Eng. Sci., 51:733-741.

[2] Desmet, G., Verelst, H., and Baron, G. V., 1996, "Local and global dispersion effects in Couette-Taylor Flow – I. Description and modeling of the dispersion effects," Chem. Eng. Sci., 51:1287-1298.

[3] Makino, T., Ohmura, N., and Kataoka, K., 2001, "Observation of isolated mixing regions in a stirred vessel," J. Chem. Eng. Japan, 34:574-578.

[4] Broomhead, D. S., and Ryrie, S. C., 1988, "Particle paths in wavy vortices," Nonlinearity, 1:409-434.

[5] Ohmura, N., Kataoka, K., Kataoka, T., and Naitoh, Y., 1997, "Vortex generation and properties of transition to turbulence in a Taylor-Couette flow system with small aspect ratio," Kagaku Kougaku Ronbunshu., 23:741-748. (in Japanese)

[6] Ottino, J. M, 1989, The kinematics of mixing: stretching, chaos and transport, Cambridge University Press, New York.